

Plasma Equilibrium Response Modelling Experiments on the JT-60U and TCV Tokamaks

J.B. Lister¹, R. Khayrutdinov², D.J.N. Limebeer⁵, V. Lukash³, Y. Nakamura⁴,
A. Sharma⁵, J.P. Wainwright⁵, R. Yoshino⁴

¹*Centre de Recherches en Physique des Plasmas, Association EURATOM-Confederation
Suisse, EPFL, 1015 Lausanne, Switzerland*

²*Triniti, Troitsk, Russian Federation*

³*RRC Kurchatov Institute, Moscow, Russian Federation*

⁴*Naka Fusion Research Establishment, JAERI, Naka, Japan*

⁵*Imperial College of Science, Technology and Medicine, London, UK*

Abstract: Experimental measurements of the plasma equilibrium dynamic response to poloidal field coil voltage variations have been performed on the JT-60U tokamak. The results have been compared with the RZIP rigid current displacement model previously validated on TCV, enhanced for this work. Although such linear response models are useful for feedback controller design, their linear time-invariant properties cannot simulate the evolution of a plasma discharge. A suitable code for this purpose is DINA, benchmarked against a complete set of experimental data from TCV control experiments in both the time and frequency domains.

DINA simulations of TCV: Considerable attention is being focused on the design of plasma position, current and shape controllers for the next generation tokamak-reactor designs like ITER-FEAT. The development of a new control algorithm for a new plasma configuration will require numerical analysis prior to experimental tests to optimise experimental time. It is therefore necessary to have a validated tokamak plasma simulator to test any new proposed plasma controller design. A first requirement of such a tool is its ability to model a real experimental plasma evolution with sufficient accuracy. Considerable success had been obtained in modelling the stationary phase of TCV discharges using two linear models, RZIP and CREATE-L. However, to simulate a full discharge we require a non-linear self-consistent model. DINA is a tokamak plasma simulation code comprising a 1.5D axi-symmetric, time-dependent, resistive MHD and transport-modelling free boundary equilibrium solver in an externally imposed magnetic field and is a suitable candidate for such work. In this paper DINA is validated against an extensive set of TCV plasma equilibrium response experiments. Initial test runs indicated that two improvements were useful. Firstly the feedback controller for these discharges has a high low-frequency gain to reduce static offset. The feedback controller had to be initialised suitably at the start of the simulation to avoid a transient which could drive the simulation unstable and even end it prematurely, Fig.1. Secondly, it is difficult to adjust the poloidal flux consumption between the experiment and the simulation, since the latter did not model the transport. Modelling the transport would not have helped since a long adjustment by trial and error would again have been necessary to obtain modest agreement. A simple solution was therefore adopted, feeding back the toroidal resistance to agree with the experiment. This adjustment did not perturb the investigation into the dynamic equilibrium response which in most cases was assessed with the lowest frequency (drift and offset) removed.

With these two improvements, a total of 27 discharges were simulated with no adjustment, with one minor numerical problem encountered for one discharge. Both limited and diverted plasmas are well modelled during the plasma current flat-top for the rejection of external square-wave PF coil voltage pulses. Examples of the comparison between TCV and DINA responses are shown in Fig.2. The agreement between the simulation and the experimental

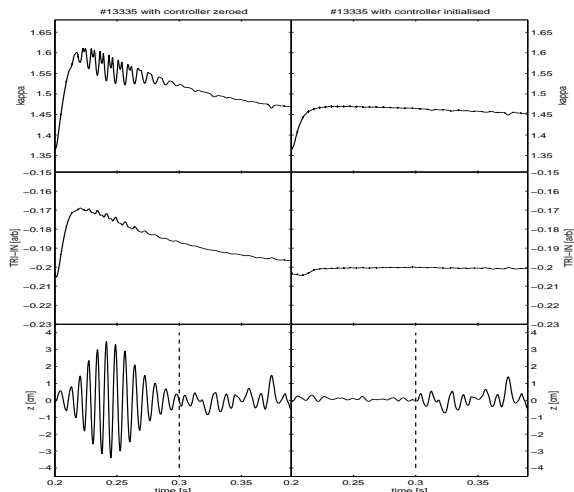


Figure 1 Improvement to the controller initialisation caused a significant reduction to the transients at the start of the DINA simulation (right). Uninitialised (left), the transient included an increase to the vertical field decay index and hence to the elongation (top trace), resulting in an anomalous vertical instability showing up on the vertical movement trace (bottom) which caused a failure of the simulation in early tests. The middle trace shows the excursion of the control parameter for elongation. The start of the stimulation is indicated as a vertical dotted line.

results is almost always within the noise width of the experimental data.

A complete single null diverted plasma discharge was also successfully simulated. The most significant difference was the penetration time of the poloidal flux, leading to a delayed onset of sawtoothing in the DINA simulation than in the experiment, Fig.3. Since the plasma loop resistance has been adjusted to the experimental data, this implies that the initial penetration of the poloidal flux does not follow the toroidal resistivity and that care should be taken in using this assumption when investigating the plasma current ramp-up phase.

Square pulse voltage stimulation of the OH1 and OH2 coils led to oscillations during the shape excursions, not reproduced by linear simulations, seen in Fig. 4 for the OH1 response. The oscillations seen in the vertical position are well reproduced by the DINA simulation. The envelope increases around 400msec, showing that the TCV closed loop has gone unstable, with a growth time of 200-400msec. After 100msec, the oscillations become damped, when the closed loop is stable again. This change in closed loop stability is attributable to the increased vertical field decay index which causes an excursion of the plasma elongation. The increase of elongation from 1.45 to 1.53 occurs when the closed loop

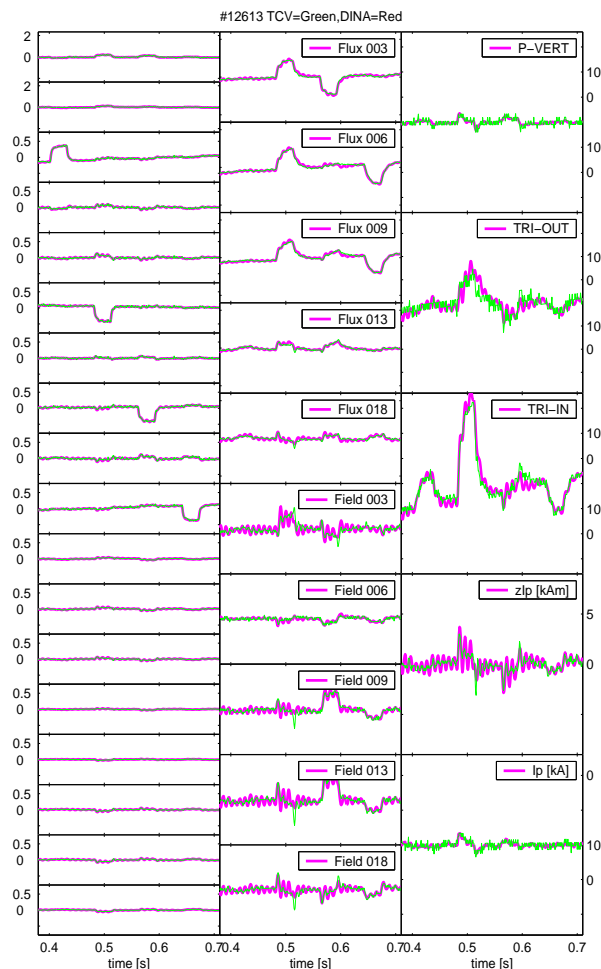


Figure 2 Simulation of a diverted off-centred plasma, using separate E1, E4, E6, E8 coil stimulations in a single pulse. The signals are shown detrended: (left column) all 18 external PF coil currents, OH1, OH2, E1 to E8, F1 to F8; (middle column) flux loops #3,6,9,13,18, magnetic probes #3,6,9,13,18; (right column) the five feedback control parameters.

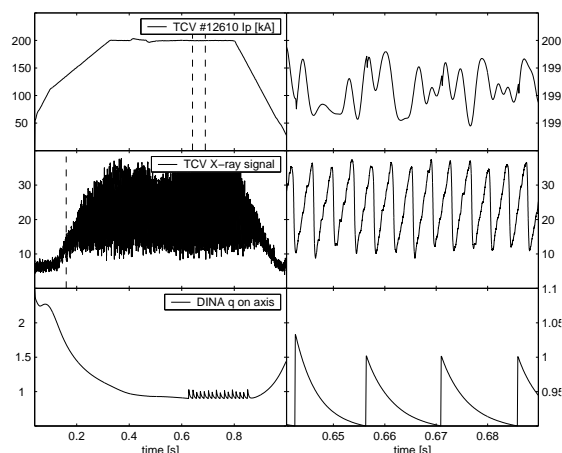


Figure 3 Comparison between DINA simulation and TCV for the evolution of the sawtooth activity: left, the full pulse showing, from top to bottom: TCV Ip, TCV soft X-ray signal, DINA $q(0)$; right, an expanded view of the same signals.

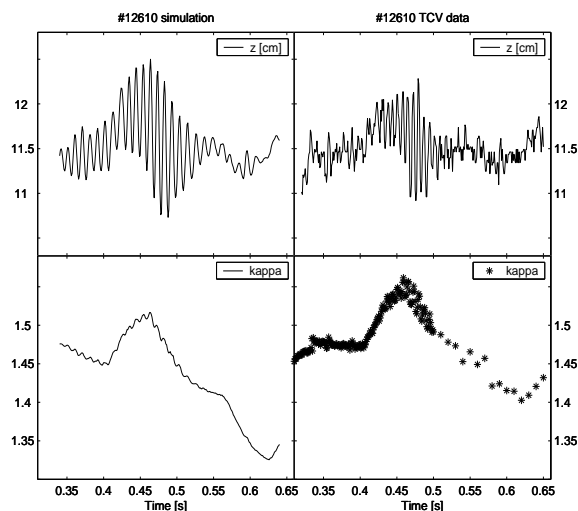


Figure 4 Comparison between TCV (left) and the DINA simulation (right) for a large excursion due to a square voltage pulse OHI stimulation. The vertical position goes closed loop unstable and returns to closed loop stable once the elongation is reduced.

is unstable. This observation is an example of non-time-invariant behaviour of the experiment and the simulation, which can never be simulated by linearised models, for which time invariance is assumed.

The complete set of 18 frequency stimulation experiments used to measure the open loop TCV plasma equilibrium response was also simulated in DINA and the results were analysed in an identical fashion to the experimental data. We used the coil voltages rather than the PF power supply demand voltages as the input signal, since this change actually renders the analysis more sensitive to differences between models, although being more noise prone. The frequency response of the DINA simulations agreed with the experimental results.

JT-60U Experiments: The method used on TCV to measure the open-loop plasma equilibrium response during the closed-loop control of the vertically unstable plasmas has been repeated on JT-60U. The RZIP model of JT-60U was created using a cleaner Lagrangian approach. This removed an asymmetry in the determining equations concerning the radial derivative of the plasma resistance, but left most terms unchanged, see below. A series of experiments was then performed with no plasma, in an Ohmic plasma and an NBI-heated plasma, using multi-sine excitation of the 5 PF coil voltages in the range 4-80Hz, to determine the dynamic response of all diagnostics. The plasma-less model was fine-tuned to compensate for external circuitry and any constructional differences, to a precision beyond simple measurement accuracy. This procedure was necessary to avoid biasing the measurements with plasma and attributing any differences to plasma model errors. The open-loop plasma response agreed well with the RZIP model, except for the plasma current response. Varying the plasma resistance derivative in the model showed that this term is not experimentally determined in these experiments. Calibrating the values of the plasma inductance and plasma resistance in the model to agree with the experimental data showed that the effective resistance is much higher than the loop resistance and that the effective inductance is somewhat lower than the low frequency inductance. It is assumed that these observations can be explained by a skin-effect.

$$\begin{bmatrix} L_s & \left. \frac{\partial M_{sp}}{\partial z} \right|_0 & \left. \frac{\partial M_{sp}}{\partial R} \right|_0 & M_{sp}^0 \\ \left. \frac{\partial M_{sp}}{\partial z} \right|_0 & \left. \frac{\partial^2 M_{sp}}{\partial z^2} \right|_0 \frac{I_s^0}{I_p^0} & \left. \frac{\partial^2 M_{ps}}{\partial z \partial R} \right|_0 \frac{I_s^0}{I_p^0} & 0 \\ \left. \frac{\partial M_{ps}}{\partial R} \right|_0 & \left. \frac{\partial^2 M_{ps}}{\partial z \partial R} \right|_0 \frac{I_s^0}{I_p^0} & \left(\frac{1}{2} \left. \frac{\partial^2 L_p}{\partial R^2} \right|_0 + \left. \frac{\partial^2 M_{ps}}{\partial R^2} \right|_0 \frac{I_s^0}{I_p^0} \right) & \left(\left. \frac{\partial L_p}{\partial R} \right|_0 + \left. \frac{\partial M_{ps}}{\partial R} \right|_0 \frac{I_s^0}{I_p^0} + 4\pi\mu_0 \frac{S}{l^2} \beta_p^0 \right) \\ M_{ps}^0 & 0 & \left(\left. \frac{\partial M_{ps}}{\partial R} \right|_0 \frac{I_s^0}{I_p^0} + \left. \frac{\partial L_p}{\partial R} \right|_0 + 4\pi\mu_0 \frac{S}{l^2} \beta_p^0 \right) & L_p^0 + 4\pi\mu_0 \frac{S}{l^2} \beta_p^0 R^0 \end{bmatrix} \vec{x} +$$

$$\begin{bmatrix} \Omega_s & 0 & 0 & 0 \\ 0 & 0 & 0 & 0 \\ 0 & 0 & 0 & \left. \frac{\partial \Omega_p}{\partial R} \right|_0 \\ 0 & 0 & \left. \frac{\partial \Omega_p}{\partial R} \right|_0 & \Omega_p^0 \end{bmatrix} \vec{x} = \begin{pmatrix} \delta V_s \\ 0 \\ -2\pi\mu_0 \frac{S}{l^2} I_p^0 \beta_p \\ -4\pi\mu_0 \frac{S}{l^2} I_p^0 R^0 \beta_p \end{pmatrix}$$

The resulting agreement is shown in Fig. 5 for the most important responses, namely the control parameters. The plasma-less response is shown as black crosses and the plasma responses as red and blue circles. The RZIP model is shown as solid lines of the same colours. Finally, the closed loop operation of JT-60U was successfully simulated using

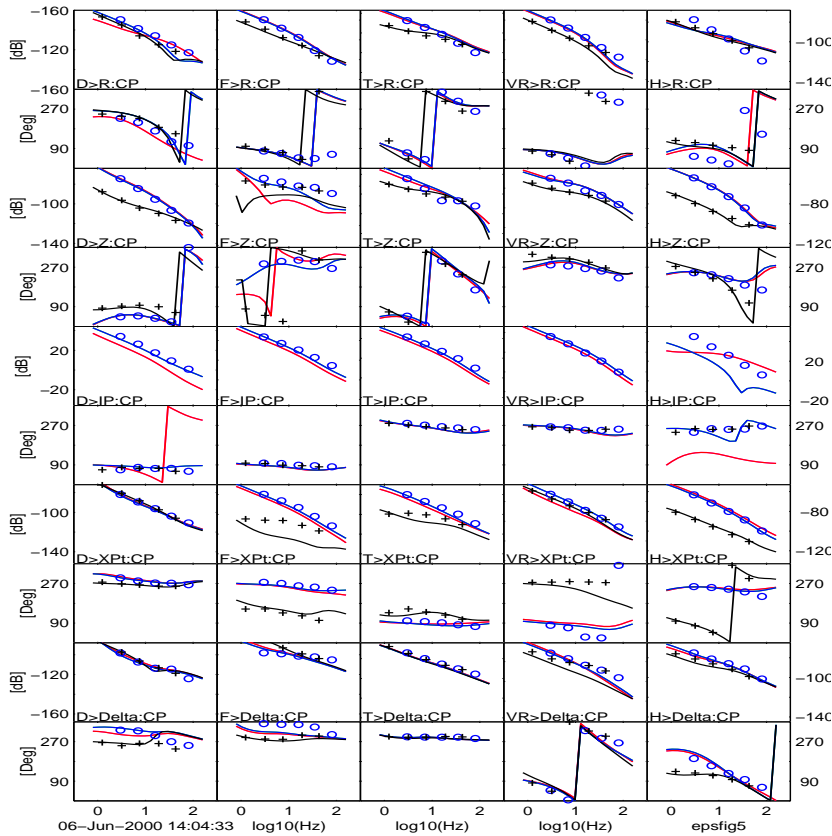


Figure 5 Selected open-loop responses from the JT-60U tokamak

the RZIP model and fine-tuning the controller to reduce some of the residual cross-coupling has started.

Acknowledgements:

Thanks go to the TCV and JT-60U teams without whom the experimental results would not be comparable with the models. Two of the authors (RK, VL) thank the CRPP for their hospitality during visits to TCV. Two of the authors (JBL, AS) thank JAERI-Naka for their hospitality during visits to JT-60U. This work was partly supported by the Swiss National Science Foundation. One of the authors (JPW) was partly supported by the United Kingdom EPSRC.